DE GRUYTER OPEN

Journal of ELECTRICAL ENGINEERING, VOL 68 (2017), NO6, 435–443

A novel power harmonic analysis method based on Nuttall-Kaiser combination window double spectrum interpolated FFT algorithm

Tao Jin*, Yiyang Chen*, Rodolfo C. C. Flesch**

Abstract Harmonics pose a great threat to safe and economical operation of power grids. Therefore, it is critical to detect harmonic parameters accurately to design harmonic compensation equipment. The fast Fourier transform (FFT) is widely used for electrical popular power harmonics analysis. However, the barrier effect produced by the algorithm itself and spectrum leakage caused by asynchronous sampling often affects the harmonic analysis accuracy. This paper examines a new approach for harmonic analysis based on deducing the modifier formulas of frequency, phase angle, and amplitude, utilizing the Nuttall-Kaiser window double spectrum line interpolation method, which overcomes the shortcomings in traditional FFT harmonic calculations. The proposed approach is verified numerically and experimentally to be accurate and reliable.

K e y w o r d s: power system, harmonic analysis, barrier effect, window function, FFT

1 Introduction

The rapid development of smart grid technologies, large applications of different kinds of nonlinear power loads and power electronic devices affect stable operation of the power grid, and the requirements of electric power measurement have continuously improved [1]. For example, a rectifier connected to the system draws a current that is not necessarily sinusoidal, and it is essential to detect, analyze, and restrain system harmonics. FFT is one of the most popular power harmonics analysis methods and can decompose the current waveform into a series of simple sinusoids. Wide area measurement systems (WAMS) are becoming more utilized in real-time measurement of network parameters, and synchronized phasor measurement unit (PMU) data can be used to support high accuracy harmonic analysis of power grids [2, 3]. However, PMUs generally measure the data asynchronously for a variety of reasons. Hence, using FFT to analyze these harmonic signals can result in large frequency, amplitude, and phase angle errors, from spectral leakage, caused by time domain truncation, and the picket fence effect, caused by frequency domain discretization. Thus, new methods must be developed to ensure correct harmonic compensation.

Polynomial windows are widely utilized to solve FFT harmonic analysis problems. Modifying and optimizing the coefficients of polynomial windows in the time domain allows the frequency responses to be easily changed [4, 5], while taking advantage of their relatively low computational complexity. They are particularly suitable for practical DSP and FPGA applications. The most widely used windows for FFT applications are Hamming, Blackman-Harris, Nuttall, Kaiser and convolution [6-9]. Rapuano and Harris researched FFT principles and characteristics, such as minimum resolution bandwidth and scalloping loss of some window functions, and discussed the reasons for of spectral leakage and FFT-related issues when estimating spectra of digitized signals [10]. Based on four-item cosine windowing using Blackman-Harris, Rife-Vincent (I), and Rife-Vincent (III) windows, an interpolated windowed FFT algorithm to improve analysis accuracy was proposed by Qian *et al* [11]. To minimize the impact of asynchronous sampling and reduce the computation load, Zeng, Teng, Cai, *et al* proposed a reliable method based on smoothing sampled data by windowing the signal with the four-term fifth derivative Nuttall (FFDN) window [12]. For some windowing methods, if one of the data acquisition instruments fails to remove system noise, high accuracy harmonic analysis cannot be obtained since the noise produces a stronger response for high dynamic range windows than with high resolution windows. Duda [13] investigated systematic errors and noise sensitivity for analytic interpolation formulas and proposed an FFT interpolation algorithm with optimal Kaiser-Bessel or Dolph-Chebyshev windowing. Kaiser windows can define a set of adjustable window functions where the proportion between the width of the main lobe and the height of the side lobe can be freely chosen and provides superior performance for multi-tone detection along with high noise immunity [14]. While Nuttall widows, have better side lobe behaviour, Kaiser windowing is able to detect critical parameters, such as phase angles, precisely [15-17]. Consequently, depending on the required accuracy, different FFT window combination methods should be employed for power system harmonic measurement and analysis [18].

Considering the side lobe characteristics of Nuttall and Kaiser windows, this paper investigates a Nuttall-Kaiser combination window function, making use of their different advantages, and proposes an improved FFT harmonic analysis method. The proposed method can successfully

* College of Electrical Engineering and Automation, Fuzhou University, Fuzhou, China, jintly@fzu.edu.cn, ** Department of Automation and Systems, Federal University of Santa Catarina, 88040-900 Florianopolis SC, Brazil

DOI: 10.1515/jee-2017–0078, Print (till 2015) ISSN 1335-3632, On-line ISSN 1339-309X

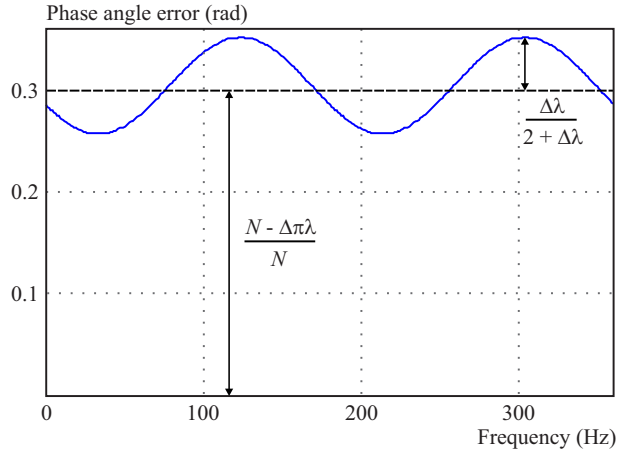

Fig. 1. Total phase angle error using DFT($N = 32$, $\Delta\lambda = 0.1$)

analyze a synchronous harmonic sampled data with high accuracy and efficiently eliminate spectral leakage and picket fence effects caused by signal processing. The performance and efficiency of the proposed harmonic analysis method were verified by simulation and experiment. This paper provides a brief review of FFT spectral leakage due to asynchronous sampling, analyses of the spectral characteristics of Nuttall and Kaiser windows, proposes the Nuttall-Kaiser window double spectrum line interpolation method, and investigates its application to harmonic analysis and assesses the proposed method performance by simulation and experiment.

2 FFT Harmonic analysis problem

The time domain representation of a sampled signal may be expressed as

$$x(n) = A\sin\Big(2\pi\frac{f_0}{f_s}n + \theta\Big), \tag{1}$$

where f_0 is the fundamental frequency, A is the amplitude, θ is the initial phase angle, f_s is the sampling frequency, and $n = 0, 1, 2, \ldots, N-1$. N is the number of sampling points. Applying a window function, $w(n)$, and continuous Fourier transform, the discrete approximation sequences of the sampled signal in frequency domain $X(f)$ can be obtained

$$X(f) = \sum_{n=-\infty}^{\infty} x(n)w(n)e^{-j2\pi f_n} = \frac{A}{2j}\Big[e^{j\theta}W\Big(\frac{2\pi(f-f_0)}{f_s}\Big) - e^{-j\theta}W\Big(\frac{2\pi(f+f_0)}{f_s}\Big)\Big]. \tag{2}$$

Ignoring the side lobe impact of the peak of negative frequency, $-f_0$, the continuous spectrum function near the positive frequency, f_0, can be expressed as

$$X_+(f) = \frac{A}{2j}e^{j\theta}W\Big(\frac{2\pi(f-f_0)}{f_s}\Big), \tag{3}$$

which may be discretely sampled, giving the discrete Fourier transform

$$X_+(k\,\Delta f) = \frac{A}{2j}e^{j\theta}W\Big(\frac{2\pi(k\Delta f - f_0)}{f_s}\Big), \tag{4}$$

where $k = 0, 1, 2, \ldots, N-1$, $\Delta f = \frac{f_s}{N}$, N is the length of data truncation, W is the frequency function of $w(n)$, and k is the coefficient of the frequency of interest f.

Phase angle is a very import parameter in power systems, both theoretically and practically, and it is critical to measure phase angle to high precision. If Δf is the frequency resolution, *ie* , the frequency deviation rate is $\Delta\lambda = \Delta f/f_0$, then the static phase angle error caused by asynchronous sampling using discrete Fourier transform (DFT) is

$$\Delta\varphi_1 = \frac{\Delta\lambda\pi(N-1)}{N} \tag{5}$$

and the dynamic phase angle error is

$$\Delta\varphi_2 \approx \frac{\sin(\pi\Delta\lambda/N)}{\sin[\pi(2+\Delta\lambda)/N]}\sin\theta. \tag{6}$$

In most situations Δf is very small, and $N > 10$, so (6) can be simplified to

$$\Delta\varphi_2 \approx \frac{\Delta\lambda}{2+\Delta\lambda}\sin\Big[2\theta + \frac{2\pi(N-1)(1+\Delta\lambda)}{N}\Big]. \tag{7}$$

Thus, phase angle static error in asynchronous conditions is proportional to the frequency deviation rate $\Delta\lambda$ and can be easily determined. However, phase angle dynamic error is not only related to $\Delta\lambda$, but also to the initial phase angle, hence the calculation is complex and

Table 1. Coefficients and characteristic parameters of four typical Nuttall window functions

Window type	Coefficients				HSSL (dB)	Side lobe decaying rate (dB/oct)
	b_0	b_1	b_2	b_3		
Minimum 3-term	0.4243801	0.4973406	0.0782793	–	–71.46	6
First order 4-term	0.3557680	0.4873960	0.1442320	0.0126040	–93.34	18
Third order 4-term	0.3389460	0.4819730	0.1610540	0.0180270	–82.73	30
Minimum 4-term	0.3635819	0.4891775	0.1365995	0.0106411	–95.89	6

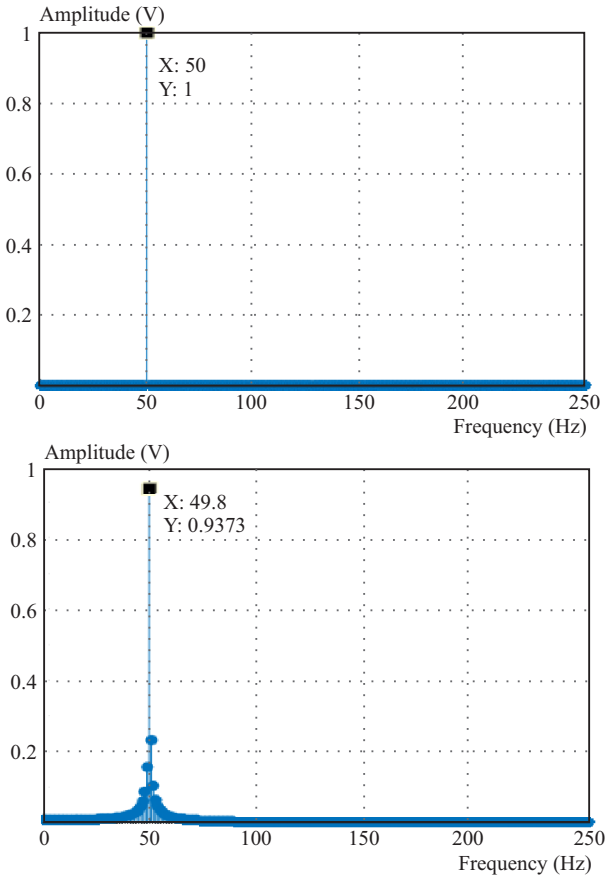

Fig. 2. Discretised spectrum analysis for sampling: (a) – synchronous sampling, (b) – asynchronous sampling

an accurate estimate is difficult. Figure 1 shows the total error of phase angle for fundamental frequency 50 Hz, in black and the dynamic error in blue.

The frequency spectrum for synchronous and asynchronous sampling based on the above analysis is shown in Fig. 2. Figure 2(a) shows that, for synchronous sampling, the spectrum peak of discrete points can accurately reflect the frequency and amplitude of the original signal. However, asynchronously sampling the signal, Fig. 2(b), causes the spectrum peak of discrete points to deviate from the actual values, in Fig. 2(b), the frequency deviation is 0.2 Hz, and amplitude deviation is 0.0627 V.

With asynchronous sampling, the signal energy is not focused at the spectrum peak spectrum, and spectral leakage will occur for FFT calculation. Thus, FFT processing is inaccurate and must be revised.

3 Proposed Nuttall-Kaiser interpolated FFT method

3.1 Spectral characteristics of Nuttall and Kaiser windows

The Nuttall window is a cosine combination window, and the discrete time domain Nuttall window can be expressed as [19]

$$w_N(n) = \sum_{m=0}^{M-1} (-1)^m b_m \cos\frac{2\pi m}{N}, \tag{8}$$

where N is the total number of samples; M is the number of terms of the window function; $n = 0, 1, 2, \ldots, N-1$ and b_m are the window coefficients, which satisfy $\sum_{m=0}^{M-1} b_m = 1$, $\sum_{m=0}^{M-1}(-1)^m b_m = 0$. Applying the discrete Fourier transform to (8), the spectrum functional expression of the Nuttall window can be expressed as

$$W_N(\omega) = \sum_{m=0}^{M-1} (-1)^m \frac{b_m}{2}\left[W_R\left(\omega - \frac{2\pi}{N}m\right) + W_R\left(\omega + \frac{2\pi}{N}m\right)\right] \tag{9}$$

where ω is the angular frequency,
$W_R(\omega) = \left(\sin\frac{N\omega}{2}/\sin\frac{\omega}{2}\right)e^{-j\frac{N-1}{2}\omega}$.

Window function coefficients have been widely researched and discussed to achieve faster decaying sidelobes and guarantee a given width of the main lobe [20, 21], and common Nuttall window functions are minimum 3-term, first order 4-term, third order 4-term, and minimum 4-term, with coefficients as listed in Table 1. Figure 3 shows the normalized magnitude frequency response curves of the above Nuttall window functions, and some characteristic parameters are also listed in Table 1.

In Fig. 3 the highest side lobe level (HSLL) for the minimum 4-term Nuttall window is 95.89 dB, with side lobe decaying rate 6 dB/oct. The HSLL for the first order 4-term window is less than the minimum 4-term (93.34 dB), but has superior side lobe decaying rate (18 dB/oct). The third order 4-term Nuttall window has HSLL = 82.73 dB, with side lobe decaying rate 30 dB/oct. Thus, the third order 4-term Nuttall window has the best side lobe characteristics, and was adopted to develop a method to suppress spectral leakage errors in harmonic analysis.

The Kaiser window can customize a set of adjustable window functions to provide superior performance for multi-tonal detection, especially for harmonic analysis, and its time domain representation can be expressed as [22]

$$w_K(n) = \frac{I_0\left(\beta\sqrt{1-\left(\frac{n}{N/2}\right)^2}\right)}{I_0(\beta)}, \tag{10}$$

where β is the shape parameter of window function, and $I_0(\beta)$ is the first class modified Bessel function. After Fourier transform, the frequency domain functional expression of the Kaiser window can be expressed written as

$$W_K(\omega) = \frac{N}{I_0(\beta)} \frac{\sinh\sqrt{\beta^2 - (N\omega/2)^2}}{\sqrt{\beta^2 - (N\omega/2)^2}}. \tag{11}$$

Applying the same $(N-1)/2$ translation as in the Nuttall window, the range satisfies $[0, N-1]$, and

$$W_K(\omega) = \frac{N-1}{I_0(\beta)} \frac{\sinh\sqrt{\beta^2 - (N-1)\omega/2}}{\sqrt{\beta^2 - (N-1)\omega/2}} e^{-j\frac{N-1}{N}\pi k}. \tag{12}$$

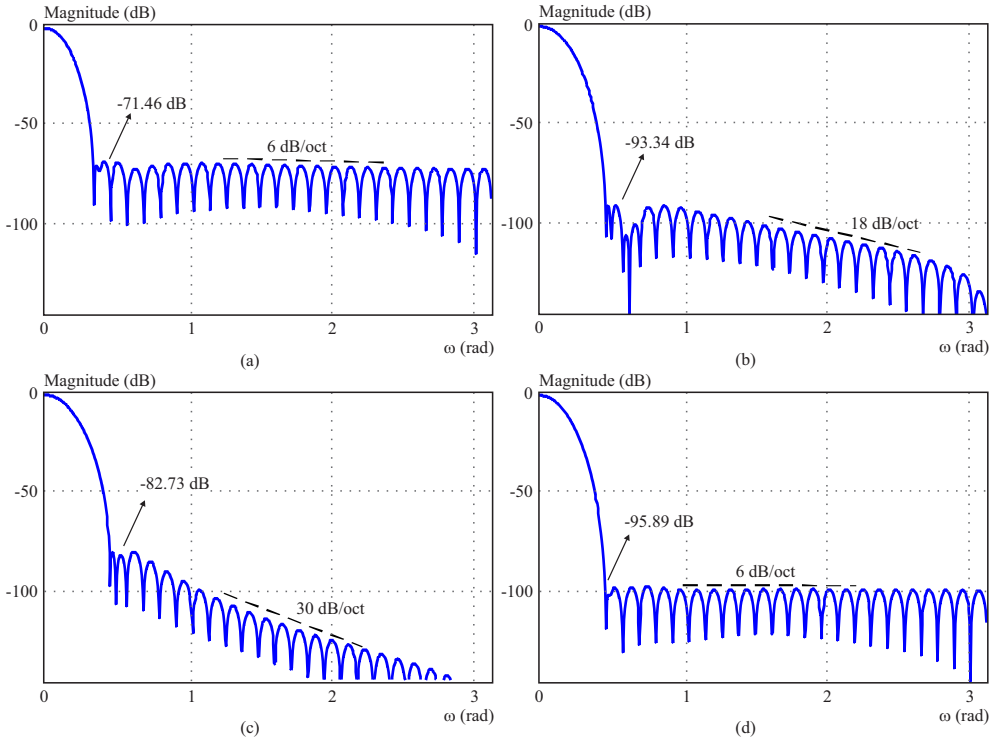

Fig. 3. Normalized logarithm spectra for Nuttall windows: (a) – minimum 3-term, (b) – first order 4-term, (c) – third order 4-term, (d) – minimum 4-term

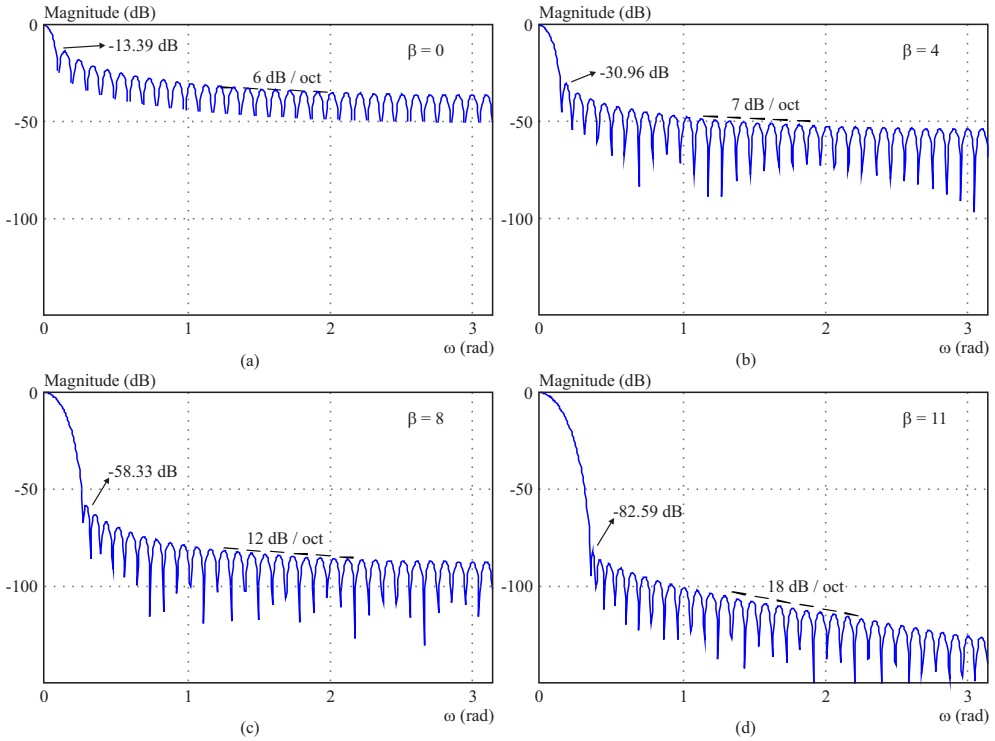

Fig. 4. Normalized logarithm spectra for Kaiser windows: (a) – $\beta = 0$, (b) – $\beta = 4$, (c) – $\beta = 8$, (d) – $\beta = 11$

Figure 4 shows the normalized logarithmic spectrum of the Kaiser window for $\beta = 0, 4, 8$, and 11. As β increases, the side lobe peaks of the Kaiser window reduce, and the decay rate increases. When $\beta = 11$, the side lobe peak is 82.59 dB, and decay rate is $= 18$ dB/oct. If continued to increase, the side lobe peaks would continue to decline, but the main lobe would widen, which would reduce the frequency resolution.

3.2 Nuttall-Kaiser window for interpolated FFT

Suppose a signal $x(t)$ contains harmonic components, with fundamental frequency, amplitude, and phase angle

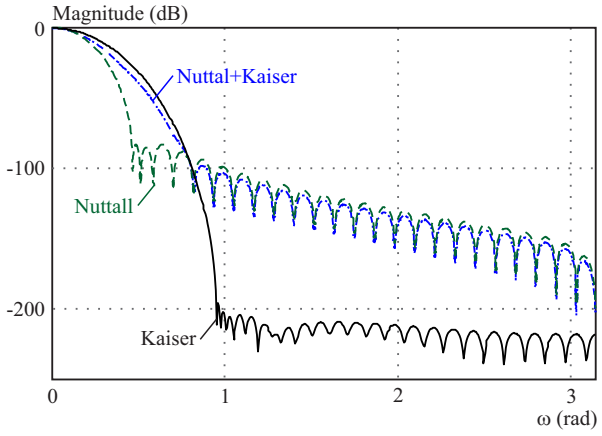

Fig. 5. Spectrum features of Nuttall, Kaiser, and Nuttall-Kaiser combination windows

Table 2. Fundamental and harmonic components of the simulated signal

Harmonic	Frequency (Hz)	Amplitude (V)	Phase (rad)
1	50.2	220	$\pi/3$
2	100.4	0.5	$\pi/3$
3	150.6	25	$\pi/3$
4	200.8	0.4	$\pi/3$
5	251.0	6	π
6	301.2	0.3	$\pi/3$
7	351.4	4	$\pi/3$
8	401.6	0.2	π
9	451.8	2	$2\pi/3$

f_1, A_1, and θ_1, respectively. Using sampling frequency f_s to obtain uniform sampling, the discrete time signal is

$$x(n) = \sum_{i=1}^{I} A_i \sin\Big(2\pi \frac{i f_1}{f_s} n + \theta_i\Big), \tag{13}$$

where i is the harmonic order. When $i \neq 1$, A_i and θ_i represent the harmonic amplitude and phase angle of the i-th harmonic, respectively. A combination Nuttall-Kaiser window function method is proposed to deal with signals such as equation (13),

$$W(\omega) = \chi \times W_N(\omega) + \gamma \times W_K(\omega)\,, \tag{14}$$

where χ, γ are the scale factors of the Nuttall and Kaiser windows, respectively. The discrete Fourier expression of the sampling signal is

$$X(k\Delta f) = \frac{A_i}{2j} e^{j\theta_i} W\Big(\frac{2\pi(k\Delta f - f_i)}{f_s}\Big). \tag{15}$$

Usually, a narrow window main lobe is desired to reduce the noise effect, but the benefit of reducing the side lobe peak is larger than the cost of the loss of frequency resolution [23]. Based on many simulations and experiments, this paper proposes utilizing the Kaiser window with $\beta = 25$, combined with the third order 4-term Nuttall window with $\chi, \gamma = 0.5$, to meet the accuracy requirement of power system harmonic analysis.

The angular frequency ω can be described as $\omega = 2\pi k/N$, then

$$W\Big(\frac{2\pi}{N}k\Big) = 0.5\Big\{\sin\pi k\, e^{-j\pi k} \times \Big[\sum_{m=0}^{M-1}(-1)^m \frac{b_m}{2} \frac{\sin\frac{2\pi k}{N}}{\sin\frac{\pi(k-m)}{N}\sin\frac{\pi(k+m)}{N}}\Big] + \frac{N-1}{I_0(\beta)} \frac{\sinh\sqrt{\beta^2 - \big[\frac{N-1}{N}\pi k\big]^2}}{\sqrt{\beta^2 - \big[\frac{N-1}{N}\pi k\big]^2}} e^{-j\frac{N-1}{N}\pi k}\Big\} \tag{16}$$

When sampling asynchronously, the peak frequency is $f_i \neq k_i\Delta f$, where k is the actual peak point corresponding to the line. Suppose the maximum spectrum line is k_{i1}, with the second largest line $k_{i2}(= k_{i1}+1)$, $k_{i1} \leq k_i \leq k_{i2}$, and y_1 and y_2 are the amplitudes of the two lines. Let $\delta = \frac{y_2 - y_1}{y_2 + y_1}$, $\alpha = k_i - k_{i1} - 0.5$, so the range of α is $(-0.5, 0.5)$, then

$$\delta = \frac{\Big|W\Big(\frac{2\pi(-\alpha+0.5)}{N}\Big)\Big| - \Big|W\Big(\frac{2\pi(-\alpha-0.5)}{N}\Big)\Big|}{\Big|W\Big(\frac{2\pi(-\alpha+0.5)}{N}\Big)\Big| + \Big|W\Big(\frac{2\pi(-\alpha-0.5)}{N}\Big)\Big|}. \tag{17}$$

Since N is generally very large, let $k = -\alpha \pm 0.5$, and equation (16) becomes

$$\Big|W\Big(\frac{2\pi(-\alpha+0.5)}{N}\Big)\Big| \approx 0.5\Big\{\Big|\sin\pi(-\alpha\pm0.5)\sum_{m=0}^{M-1}(-1)^m\frac{b_m}{\pi}\frac{N(-\alpha\pm0.5)}{(-\alpha\pm0.5)^2-m^2}\Big| + \Big|\frac{N-1}{I_0(\beta)}\frac{\sinh\sqrt{\beta^2-(\pi k)^2}}{\sqrt{\beta^2-(\pi k)^2}}\Big|\Big\}, \tag{18}$$

where the frequency modifier formula is

$$f_i = k_i\Delta f = (\alpha + k_{i1} + 0.5)\Delta f\,. \tag{19}$$

Thus, the amplitude correction is

$$A_i = \frac{A_{i1}\Big|W\big(\frac{2\pi(k_{i1}-k_i)}{N}\big)\Big| + A_{i2}\Big|W\big(\frac{2\pi(k_{i2}-k_i)}{N}\big)\Big|}{\Big|W\big(\frac{2\pi(k_{i1}-k_i)}{N}\big)\Big| + \Big|W\big(\frac{2\pi(k_{i2}-k_i)}{N}\big)\Big|} = \frac{2(y_1+y_2)}{\Big|W\big(\frac{2\pi(-\alpha+0.5)}{N}\big)\Big| + \Big|W\big(\frac{2\pi(-\alpha-0.5)}{N}\big)\Big|} \tag{20}$$

where A_{i1} is the amplitude of k_{i1}, A_{i2} is the amplitude of k_{i2}.

As above, N is usually large, so using the polynomial fitting approximation, the simplified amplitude value is

$$A_i = \frac{y_1 + y_2}{N}\, g(\alpha) \tag{21}$$

and the phase angle correction for the combination window is

$$\theta_i = \arg\left[X(k_{i1}\Delta f)\right] + \frac{\pi}{2} - \arg\Big[W\big(\frac{2\pi(k_{i1}\Delta f - f_i)}{f_s}\big)\Big], \tag{22}$$

Table 3. Relative amplitude errors

	Amplitude estimation relative errors $\times 10^6$								
Window	ΔA_1	ΔA_2	ΔA_3	ΔA_4	ΔA_5	ΔA_6	ΔA_7	ΔA_8	ΔA_9
Nuttall	0.46	211.68	1.03	1262.22	2.16	0.90	159.12	1.43	1044.99
Kaiser	0.09	42.00	0.20	254.89	0.42	0.17	31.41	0.27	210.40
Nuttall-Kaiser	0.07	99.97	0.67	608.51	1.04	0.13	75.02	0.87	502.43

Table 4. Relative phase angle errors

	Relative errors of phase angle estimation $\times 10^6$								
Window	ΔA_1	ΔA_2	ΔA_3	ΔA_4	ΔA_5	ΔA_6	ΔA_7	ΔA_8	ΔA_9
Hamming	2372.65	2183.59	1251.37	1655.04	44.19	2541.57	972.63	449.30	1040.89
Blackman-Harris	2370.26	3556.04	1262.27	4086.23	74.09	2788.36	1071.12	1036.32	1127.82
*Nuttall	2362.14	17343.54	1294.06	13766.50	207.22	4124.66	1563.27	3797.37	1649.41
Rife-Vincent 4-I	2371.88	1115.59	1256.25	2231.25	46.87	2512.50	975.00	465.62	1045.31
Nuttall-Kaiser	2880.05	1348.31	1519.80	2584.08	54.80	3052.06	1179.16	563.64	1220.05

*minimum side lobe

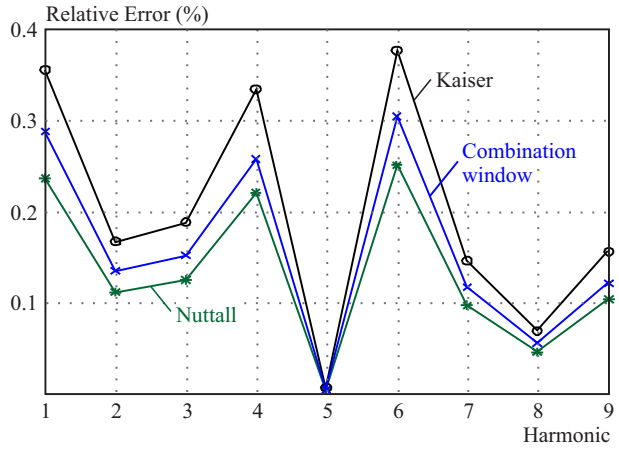

Fig. 6. Relative phase angle errors for Nuttall, Kaiser, and Nuttall-Kaiser combination of windows

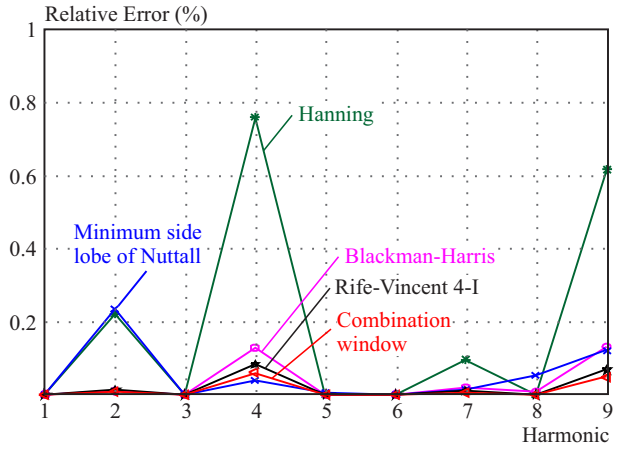

Fig. 7. Relative amplitude errors for different windows

For the proposed Nuttall-Kaiser combination window, the Kaiser window shape parameter is $\beta = 25$, and we use the third order 4-term Nuttall window, with range $\alpha = -0.49$ to $+0.49$, varied every 0.001. Substituting these values into the equations, a set of δ and $g(\alpha)$ can be obtained. Using a polynomial fit, the optimal combination window coefficients can be obtained as follows:

- Third order 4-term Nuttall window
  $\alpha = 0.0922872370\beta^5 + 0.1767199245\beta^3 + 2.9549451336\beta$,
  $g(\alpha) = 0.1472993230\alpha^4 + 0.9187462015\alpha^2 + 3.2097613145$.
- Kaiser window ($\beta = 25$)
  $\alpha = 0.2883590681\beta^5 + 0.6405439881\beta^3 + 5.2774745762\beta$,
  $g(\alpha) = 0.0661584096\alpha^4 + 0.7247717487\alpha^2 + 4.2082828094$.
- Combination Nuttall-Kaiser window
  $\alpha = 1.2618269186\beta^5 + 1.0368877011\beta^3 + 3.6499846828\beta$
  $g(\alpha) = 0.1068160200\alpha^4 + 0.8628506225\alpha^2 + 3.6418169592$.

Figure 5 shows normalized logarithmic spectra of Nuttall, Kaiser ($\beta = 25$), and proposed Nuttall-Kaiser combination windows. Windows with a narrow main lobe have better noise immunity, and the proposed combination window has better noise immunity than the Kaiser window, but also improved side lobe features than the Nuttall window. Thus, the proposed window will provide good accuracy for most power system harmonic analysis conditions.

4 Simulations and Experiments

4.1 Simulation Case Analysis

To verify the performance of the proposed Nuttall-Kaiser combination window interpolated FFT method, a 9-th harmonic signal model was used for simulations,

$$x(n) = \sum_{i=1}^{9} A_i \sin\left(2\pi \frac{if_1}{f_s} n + \theta_i\right). \qquad (23)$$

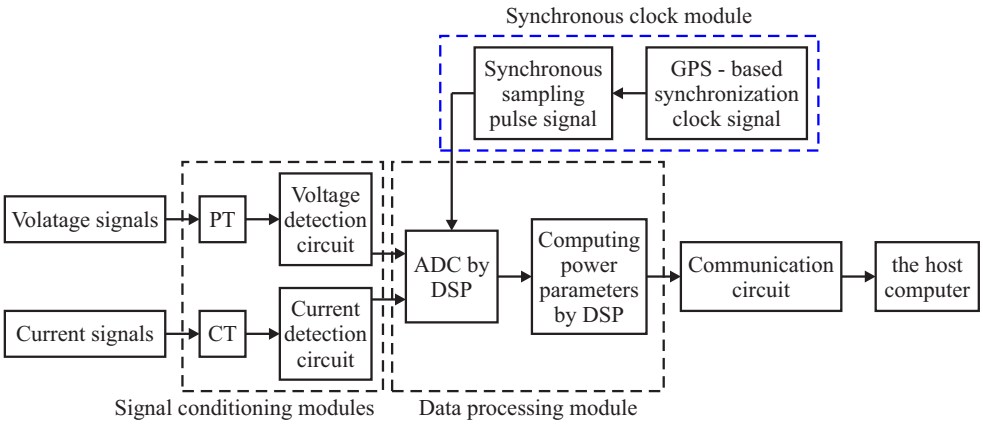

Fig. 8. Hardware diagram of experiments

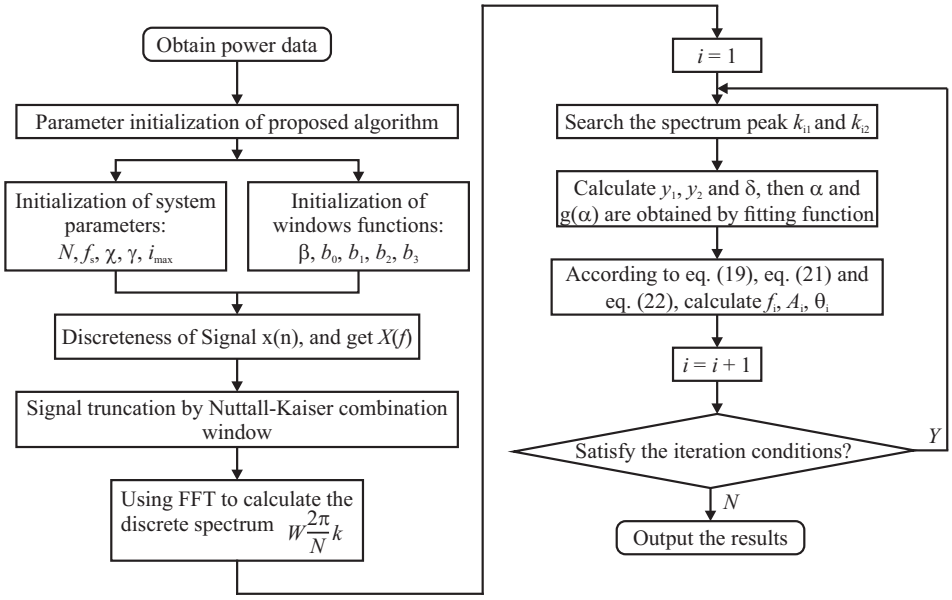

Fig. 9. Flowchart of the proposed Nuttall-Kaiser harmonic analyzing algorithm

From the GB/T 15945-2008 standard of China, the frequency deviation limit for power systems is ±0.2 Hz under normal operating conditions, so this paper considers the extreme condition, 50.2 Hz, as the fundamental frequency f_1. The sampling frequency was 1000 Hz, data length of the truncated signal $N = 1024$, and f_i, A_i and θ_i represent harmonic frequency, amplitude, and phase angle, respectively. The fundamental and harmonic components of the simulated signal are shown in Table 2.

Nuttall, Kaiser, and the proposed Nuttall-Kaiser combination windows were used to process the simulation signal, with the results shown in Table 3 and Fig. 6. The amplitude error of the Nuttall window is larger than the Kaiser and Nuttall-Kaiser combination windows, although the phase angle error is smaller. The Nuttall window has minimum phase angle error and the Kaiser window has minimum amplitude error, so it follows that the proposed Nuttall-Kaiser combination window integrates their advantages, providing good amplitude as well as good phase angle estimations.

For the same simulated signal, all three window systems provide good frequency estimates. For example, the relative error of the fundamental wave frequency provided by the proposed Nuttall-Kaiser combination window is lower than $0.8141 \times 10^{-6}\,\%$. The 4th harmonic produces the largest relative error, but it is still lower than $20.3625 \times 10^{-6}\,\%$.

To show the effects further, comparisons between different windows as Hamming, Blackman-Harris, Minimum sidelobe of Nuttall, Rife-Vincent 4-I, and the Nuttall-Kaiser combination window have also been made in Fig. 7 and Table 4. From the figure and table, although Rife-Vincent 4-I window exhibits the highest sidelobe decay rate among all cosine windows, it can be concluded that when it is taken amplitude and phase angle together the proposed Nuttall-Kaiser combination window has better performance than others [24].

Real measurements are always corrupted by noise. always noise signals doping the actual signals, which interferes with the measurement results. Therefore, to inves-

tigate systematic errors and noise sensitivity, we added white Gaussian noise with 45 dB of signal to noise ratio was added to the simulation signal model in Table 2 and tested the performance of the proposed Nuttall-Kaiser combination window interpolation FFT method was evaluated. Table 5 shows the relative errors.

The proposed method still provides high accuracy and good performance in this noisy environment, with reliable accuracy at 3, 5, and 7th harmonics.

Table 5. Relative frequency, amplitude, and phase errors for the proposed Nuttall-Kaiser combination window

Harmonic	Relative errors of Frequency (%)	Amplitude ($\times 10^2$ %)	Phase ($\times 10^2$ %)
1	0.00049798	0.00031259	0.00423752
2	0.01377363	0.05061023	0.18528018
3	0.00130134	0.00088214	0.00896885
4	0.23410102	0.0561084	1.45858127
5	0.00111195	0.01129458	0.00201986
6	0.03878151	0.29010884	0.25090039
7	0.00025585	0.00304216	0.01170572
8	0.05228783	0.16742284	0.29721858
9	0.01844717	0.04743541	0.11619199

4 Experiment and discussion

To verify the proposed Nuttall-Kaiser combination window double spectrum line interpolation FFT harmonic analysis method, harmonic signals were obtained from a Chinese grid, as where the fundamental frequency is 50 Hz and the standard voltage is 220 V. The power detection hardware which is utilized to detect the power signal is described in Fig. 8. In this device, in order to obtained high accuracy, a synchronous clock module is added to the hardware system.

The proposed algorithm flowchart is shown in Fig. 9. After obtaining the power data, the algorithm initializes the parameters, including system parameters and window functions' parameters, such as sampling points N, sampling frequency f_s, coefficients of Nuttall window b_0, b_1, b_2, b_3, and the shape parameter of Kaiser window β. Before using FFT to calculate the discrete spectrum $W\left(\frac{2\pi}{N}k\right)$, the discrete power data $X(f)$ was be truncated by the proposed Nuttall-Kaiser combination window function.

The following steps show how to use the double spectrum line method to obtain the optimal parameters of the proposed algorithm. When the maximum spectrum line k_{i1} and the second largest line k_{i2} are found at arbitrary integer harmonics in real-time detection, their amplitudes can be calculated as y_1, y_2. By (17), parameter δ is gotten, then α and $g(\alpha)$ can be obtained by polynomial fitting. Utilizing equation (19), (21), and (22), the harmonic frequency f_i, amplitude A_i and phase angle θ_i will be calculated. After a series of iterations, the optimal solutions of harmonic analysis will be reached. The key issue of the proposed algorithm is to get α and $g(\alpha)$ in the iterations.

Figure 10 shows that for traditional FFT spectrum analysis, since the harmonic signal is complex and includes many different types of noise, only frequencies near 50 Hz and 150 Hz can be analysed clearly because of the low harmonic amplitude.

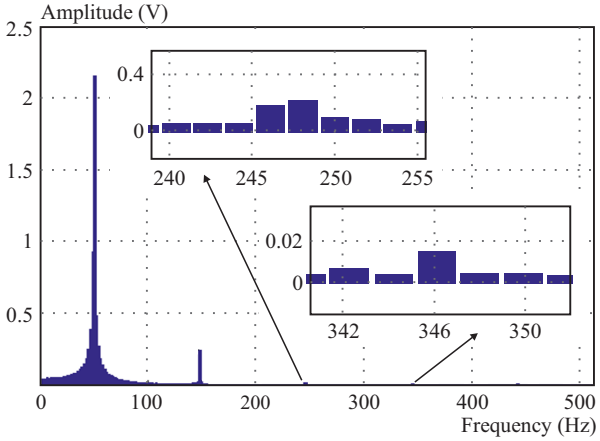

Fig. 10. Traditional FFT spectrum analysis of the signal shown in Fig. 8

The proposed Nuttall-Kaiser combination window interpolation FFT harmonic analysis method provides superior amplitude, frequency, and phase angle estimates than the traditional FFT harmonic analysis method. Table 5 shows the frequency analysis for the traditional and proposed methods. The actual harmonic signal includes mainly the fundamental, 3, 5, and 7th harmonics. The relative fundamental frequency error by traditional FFT is 0.02 %, whereas for the proposed method it is 0.0022 %. The same analysis for the 5th harmonic results in an error of 0.8% for the traditional method and 0.1489% for the proposed method. Thus, the proposed method provides superior estimate accuracy than the traditional FFT harmonic analysis method.

5 Conclusions

This paper analyzed features of Nuttall and Kaiser windows, and showed they have good resistance to spectrum leakage caused by asynchronous non-integer discretization. The Nuttall window has higher phase angle precision with lower amplitude precision compared to the Kaiser window model. Therefore, this paper proposed a combination windowing model, combining the Nuttall and Kaiser window advantages to obtain more reliable estimates of harmonic amplitude and phase angle. Experimental results verified the proposed method has better stability and reliability. For non-integer discretization, the relative error of the fundamental frequency is lower than 0.815×10^{-6} %, while the amplitude error of the

Table 6. Frequency estimates from the signal shown in Fig. 8

		FFT		Nuttall-Kaiser window	
Harmonic order	Frequency (Hz)	Actual value (Hz)	Relative error (%)	Actual value (Hz)	Relative error (%)
1	50	49.9	0.02	50	0.0022
3	150	148.1	1.27	150	0.0078
5	250	248	0.80	250	0.1489
7	350	346	1.14	350	0.1019

9th harmonic is lower than 0.051 %, and phase angle error is lower than 0.123 %. Future research work will focus on how to improve the combination window resolution in complex power environments.

Acknowledgements

This work was primarily supported by the European Community 7th Framework Programme (Grant 909880), Chinese National Natural Science Foundation (Grant 61304260), and Fujian Science Foundation for Distinguished Young Scholars (Grant 2012J06012). The authors would like to thank the reviewers for their advice and suggestions on improving the paper.

References

[1] D. Belega and D. Petri, "Accuracy Analysis of the Multi Cycle Synchrophasor Estimator Provided by the Interpolated DFT Algorithm", *IEEE Trans. Instrum. Meas.*, 2013, vol. 62, no. 5, pp. 942–953.

[2] D. L. Ree, V. C. Centeno, J. S. Thorp and A. G. Phadke, "Synchronized Phasor Measurement Applications Power Systems", *IEEE Trans. Smart Grid*, 2010, vol. 1, no. 1, pp. 20–27.

[3] T. Xia and Y. L. Liu, "Single-Phase Angle Measurements Electric Power Systems", *IEEE Trans. Power Electr.*, 2010, vol. 25, no. 2, pp. 844–852.

[4] S. K. Jain and S. N. Singh, "Low Order Dominant Harmonic Estimation Using Adaptive Wavelet Neural Network", *IEEE Trans. Ind. Electron.*, 2014, vol. 61, no. 1, pp. 428–435.

[5] V. K. Jain, W. L. Collins and D. C. Davis, "High Accuracy Analog Measurements via Interpolated FFT", *IEEE Trans. Instrum. Meas.*, 1979, vol. 28, no. 2, pp. 113–122.

[6] K. M. Mottaghi and M. G. Shayesteh, "New Efficient Window Function, Replacement for the Hamming Window", *IET Signal Proc.*, 2011, vol. 5, no. 5, pp. 499–505.

[7] J. Barros and R. I. Diego, "On the Use of the Hamming Window for Harmonic Analysis the Standard Frame-Work", *IEEE Trans. Power Deliv.*, 2006, vol. 21, no. 1, pp. 538–539.

[8] H. Wen, Z. S. Teng, C. C. Li, J. D. He and S. S. Wei, "Harmonic Analysis Algorithm based on Nuttall Window and its Application Power Measurement", *Chinese Journ. Scient. Instrum.*, 2009, vol. 30, no. 9, pp. 1823–1828.

[9] A. H. Nuttall, "Generation of Dolph-Chebyshev Weights via Fast Fourier Transform", *Proc. IEEE*, 1974, vol. 62, no. 10, pp. 1396–1396.

[10] S. Rapuano and F. J. Harris, "An Introduction to FFT and Time Domain Windows", *IEEE Instrum. Meas. Mag.*, 2007, vol. 10, no. 6, pp. 32–44.

[11] H. Qian, R. X. Zhao and T. Chen, "Interharmonics Analysis based on Interpolating Windowed FFT Algorithm ", *IEEE Trans. Power Deliv.*, 2007, vol. 22, no. 2, pp. 1064–1069.

[12] B. Zeng, Z. S. Teng, Y. L. Cai, S. Y. Guo and B. Y. Qing, "Harmonic Phasor Analysis based on Improved FFT Algorithm", *IEEE Trans. Smart Grid*, 2011, vol. 2, no. 1, pp. 51–59.

[13] K. Duda, "DFT Interpolation Algorithm for Kaiser-Bessel and Dolph-Chebyshev Windows", , *IEEE Trans. Instrum. Meas.*, 2011, vol. 60, no. 3, pp. 784–790.

[14] Y. P. Gao, Z. S. Teng and B. Y. Qing, "Harmonic Analysis based on Kaiser Window Double Spectrum Line Interpolation FFT", *Chinese Journ. Scient. Instrum.*, 2010, vol. 32, no. 2, pp. 287–292.

[15] K. K. Parhi and M. Ayinala, "Low-Complexity Welch Power Spectral Density Computation", *IEEE Trans. Circuits. Syst.*, 2014, vol. 61, no. 1, pp. 172–182.

[16] H. Wen, Z. Meng, S. Guo, F. Li and Y. Yang, "Harmonic Estimation using Symmetrical Interpolation FFT based on Triangular Self-Convolution Window", *IEEE Trans. Ind. Informat.*, 2014, vol. 11, no. 1, pp. 16–26.

[17] K. F. Chen and S. L. Mei, "Composite Interpolated Fast Fourier Transform with the Hamming Window", *IEEE Trans. Instrum. Meas.*, 2010, vol. 59, no. 6, pp. 1571–1579.

[18] W. Y. Yao, Z. S. Teng, Q. Tao and Y. P. Gao, "Measurement of Power System Harmonic based on Adaptive Kaiser Self-Convolution Window", *IET Gener. Transm. Dis*, 2016, vol. 10, no. 2, pp. 390–398.

[19] B. Y. Qing, Z. S. Teng, Y. P. Gao and H. Wen, "An Approach for Electrical Harmonic Analysis based on Nuttall Window Double-Spectrum-Line Interpolation FFT", *Proc. CSEE*, 2008, vol. 28, no. 25), pp. 153–158.

[20] B. Daniel and P. Dario, "Sine-Wave Parameter Estimation by Interpolated DFT Method based on New Cosine Windows with High Interference Rejection Capability", *Digit. Signal Proc.*, 2014, vol. 33, pp. 60–70.

[21] M. D. Kusljevic, "Simultaneous Frequency and Harmonic Magnitude Estimation using Decoupled Modules and Multirate Sampling", *IEEE Trans. Instrum. Meas.*, 2010, vol. 59, no. 4), pp. 954–962.

[22] M. Nilchian, J. P. Ward, C. Vonesch and M. Unser, "Optimized Kaiser-Bessel Window Functions for Computed Tomography", *IEEE Trans. Imag. Proc.*, 2015, vol. 24, no. 11), pp. 3826–3833.

[23] F. Sh. Zhang, Zh. X. Geng and W. Yuan, "The Algorithm of Interpolating Windowed FFT for Harmonic Analysis of Electric Power System", *IEEE Trans. Power Deliv.*, 2001, vol. 16, no. 2), pp. 160–164.

[24] D. Agrez, T. Lusin and D. Ilic, "Nonparametric Estimation of the Phase Difference using RV1 and MSL Windows", *IEEE Trans. Instrum. Meas.*, 2015, vol. 64, no. 6), pp. 1405–1412.

Received 13 March 2017